J Mater Sci (2009) 44:1633–1640
DOI 10.1007/s10853-009-3246-9

Preparation of silicon carbide fibers from the blend of solid and liquid polycarbosilanes

**Ming Tang · Zhaoju Yu · Yuxi Yu ·
Litong Zhang · Lifu Chen**

Received: 17 October 2008 / Accepted: 5 January 2009 / Published online: 27 January 2009

Abstract A highly branched liquid polycarbosilane (LPCS) was added into a solid polycarbosilane (PCS) to give a polymer blend. It was then melt-spun into precursor fibers, oxidation-cured in hot-air, and converted into ceramic fibers by pyrolysis under nitrogen. It was found that the addition of the LPCS resulted in a significant drop on the spinning temperature from 285 °C (without LPCS) to 225 °C (with 15% LPCS), while the spinning ability of the polymer blend was also markedly improved over the solid PCS. Furthermore, the LPCS enhanced the oxidation curing, reducing the curing temperature and hence the tendency for fiber partial melting and sticking. However, the strength of the silicon carbide fibers decreased owing to the presence of the LPCS. The effects of the LPCS addition and their mechanisms on the fiber processing and properties were studied using FTIR, NMR, GPC, XRD, SEM, and elemental analysis.

Introduction

Silicon carbide (SiC) fiber is noticeable for its high tensile strength, excellent oxidation resistance, and thermal stability at elevated temperature. A method was developed by Yajima et al. [1–3] for the preparation of small-diameter SiC fibers. Solid polycarbosilane (PCS) was first synthesized and melt-spun into precursor fibers. The as-spun fibers were rendered infusible by oxidation curing in hot air, and then pyrolyzed under inert atmosphere to yield SiC fibers [4, 5]. One of the most important applications of SiC fibers is as the reinforcements in fiber-reinforced composites [6, 7]. For this purpose, the fibers are normally weaved into the shape of the final component and then the resultant pre-form is filled with the matrix material. To facilitate the weaving process, fibers with small diameter are desired. The reduction in fiber diameter is realized by increasing the drawing ratio during spinning. Solid PCS resembles rosin in many properties. Because of its rather low molecular weight, it is very brittle and weak. As a consequence, PCS has poor spinning ability and the fibers tend to break when excessive drawing is applied, making it very difficult to obtain continuous and small-diameter fibers. This problem becomes more conspicuous when a fiber bundle containing a large number of filaments (>500) is spun as required in practical applications. Addition of plasticizer into PCS has been used by Idesaki and co-workers [8–10] to improve the spinning ability of the PCS. In their work, 20% liquid polyvinylsilane (PVS) was added into PCS. Because of the improved spinning ability of the precursor, the average fiber diameter was markedly reduced from 11.8 to 8.5 μm. Meanwhile, the melt-spinning temperature was lowered from 320 °C (pure PCS) to 220 °C (with 20% PVS), making the spinning practice more controllable. However, the different structure between PCS and PVS (see Fig. 1) makes them incompatible. To obtain a homogeneous blend, the PVS and PCS were first dissolved in benzene. The solution was then freeze-dried to prevent phase separation during the solvent removal. This drying practice makes PVS less attractive for large-scale application.

M. Tang
Department of Materials Science and Engineering, College of Chemistry and Chemical Engineering, Xiamen University, Xiamen 361005, China

M. Tang · Z. Yu · Y. Yu · L. Zhang · L. Chen (✉)
Advanced Materials Laboratory, Department of Materials Science and Engineering, College of Materials, Xiamen University, Xiamen 361005, China
e-mail: lfchen@xmu.edu.cn

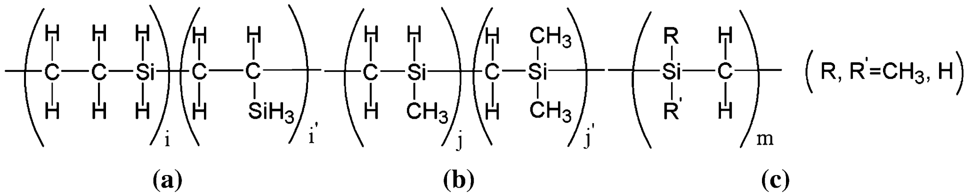

Fig. 1 Chemical formula of (**a**) polyvinylsilane (PVS), (**b**) polycarbosilane (PCS), and (**c**) liquid polycarbosilane (LPCS)

In this work, a highly branched liquid polycarbosilane (LPCS), which has a backbone chain resembling solid PCS (see Fig. 1), had been used as the spinning agent. Its effects on spinning, oxidation curing, and mechanical properties are studied. The underlining mechanisms are examined.

Experimental

Preparation of precursor fibers

Solid polycarbosilane (PCS) was synthesized following the work by Yajima et al. [1–3]. It has a number average molecular weight (M_n) of 1,400 and a melting point of 220 °C. Liquid polycarbosilane (LPCS) was prepared following the procedures described elsewhere [11]. Briefly, LPCS was synthesized by Grignard coupling of chloromethyldichloromethylsilane ($Cl_2(CH_3)SiCH_2Cl$) and chloromethyltrichlorosilane (Cl_3SiCH_2Cl), followed by the reduction with lithium aluminum hydride ($LiAlH_4$); it is a yellowish viscous liquid having a M_n of 570. The chemical formula of LPCS is shown in Fig. 1. Clearly the LPCS is rich in Si–H bonds in comparison with PCS.

The flowchart for the preparation of SiC fibers in this work is shown in Fig. 2. The solid PCS and LPCS were dissolved in hexane to give a clear yellowish solution. It was then vacuum-dried at 60 °C. The resultant polymer blend was a white powder at room temperature. The LPCS content in the blend was 2.5, 5, 10, 15, and 20% by mass on the base of the solid PCS, and the samples are abbreviated as PCS-2.5, PCS-5, PCS-10, PCS-15, and PCS-20 correspondingly. Unlike PVS, the addition of LPCS does not require freeze-drying, because of the better structural similarity between the LPCS and solid PCS, hence better compatibility.

The precursor was charged into the reservoir of a laboratory piston-type melt-spinning machine (MMCH05, Chemat, Northridge, CA). It was then heated to the melt-spinning temperature under the protection of high-purity nitrogen to prevent the precursor from oxidation. The polymer melt was extruded through a single-hole spinneret. The diameter of the orifice was 0.3 mm. To assess the spinning ability of the precursor, the rate of extrusion was kept unchanged (i.e., the lowering rate of the piston was kept constant), and the winding speed was fixed at 400 m min^{-1} to obtain the precursor fibers. The length of continuous fibers without any fiber breakage during the melt spinning was used to compare the spinning ability of the different precursors.

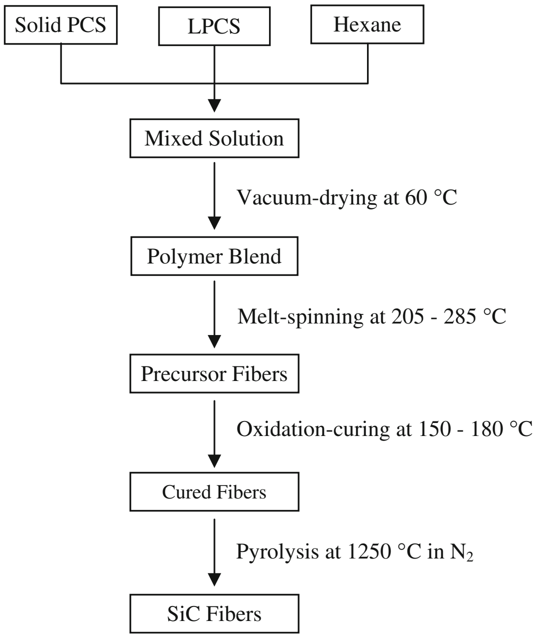

Fig. 2 Flowchart for the preparation of SiC fibers

Preparation of oxidation-cured fibers

About 0.5 g of the as-spun polymer fibers was cut into 60 mm length and then placed into a tube furnace (ID = 35 mm). The fibers were heated at a ramp rate of 10 °C h^{-1} to 150, 160, 170 and 180 °C, and maintained for 1 h to give oxidation-cured fibers with different oxygen content. The oxidant was dry air, flowing at 200 cm^3 min^{-1}.

Preparation of SiC fibers

The cured fibers were placed into a perforated graphite boat. They were then heated in high-purity nitrogen to 1250 °C at a ramp rate of 5 °C min^{-1} and maintained for 5 min. This pyrolysis converted the yellowish cured fiber into lustrous black ceramic fibers.

Analysis and characterization

FTIR and ^1H NMR were used for the analysis of chemical structure. For FTIR analysis, the spectra were recorded on

Nicolet Avator 360 (Nicolet Instrument Corporation, USA) with KBr plates for liquid samples and KBr discs for solid samples. For ^{1}H NMR analysis, the sample was dissolved in $CDCl_3$ and trimethylsilylsilane (TMS) was used as the standard. A Bruker AV300 MHz spectrometer (Bruker Corporation, Switzerland) was used, operating at the frequency of 300.13 MHz and with the delay time of 30 s.

Molecular weight and molecular weight distribution were analyzed using gel permeation chromatography (GPC) (Agilent 1100 system, Agilent Corporation, USA). The analysis was performed at 35 °C with tetrahydrofuran (THF) as the eluant (1.0 mL min^{-1}) and narrow-molecular weight-distribution polystyrene as the standard. The melting point was measured using a melting point apparatus (WRS-2A, Shanghai Precision & Scientific Instrument Co., Ltd., China). The heating rate was 5 °C min^{-1}. Five measurements were made for each sample and the average was taken as the melting point. The gel fraction of the oxidation-cured fibers was measured by Soxhlet extraction method. The fiber sample was wrapped in stainless steel gauze and extracted at 150 °C for 24 h with xylene as the eluant. After the extraction, the sample was dried and weighed. The gel fraction of the oxidation-cured fibers was calculated using the following expression: $\mathrm{Gel}\% = (w_2 - w_1)/w_1 \times \%$, where w_1 and w_2 were the weight of the sample before and after the extraction, respectively. Carbon content was determined using Horiba Carbon/Sulfur Analyzer EMIA-320V (Horiba Ltd., Japan). Oxygen content was determined using Horiba Oxygen Nitrogen Analyzer EMGA-620W (Horiba Ltd., Japan).

The tensile strength of single SiC fibers was measured using a tensile testing machine (YG(B)003A, Wenzhou Darong Textile Instrument Co., Ltd., China). The gage length was 25 mm and the crosshead speed was 1 mm min^{-1}. At least 20 fibers were tested, and the average was used. Scanning electron microscopy (XL30, Philips-FEI, Eindhoven, the Netherlands) was used for fiber diameter determination and microstructure examination. Phase identification was carried out by X-ray diffraction (XRD) (PANalytical X'Pert PRO diffractometer, PANalytical Corporation, the Netherlands) with CuK_α radiation. The samples were continuously scanned from 10° to 90° (2θ) at a speed of 0.0167 s^{-1}.

Results and discussion

Effects of LPCS on the thermal stability of the precursors

Good thermal stability is the prerequisite for a precursor when melt-spinning is used for fiber shaping. It is essential that no significant changes occur during spinning with respect to the chemical and physical properties of the precursor, such as molecular weight and melting point. In large-scale production, the whole spinning process normally lasts for hours. To evaluate the thermal stability, the polymer blend was kept at the spinning temperature for 5 h prior to melt-spinning in this work. Figure 3 shows FTIR spectra of the PCS-0, LPCS, and PCS-15 precursors. The absorption peaks are assigned on the base of the data for the known organic compounds and PCS [12–15]. The absorptions at 600–920, 1250 cm^{-1} are attributed to $Si–CH_3$, 1020 and 1355 cm^{-1} to $Si–CH_2–Si$, 2100 cm^{-1} to Si–H, and 1400, 2900, and 2950 cm^{-1} to C–H. The deformation vibration band of SiH_2 and SiH_3 in LPCS appears at 890 cm^{-1}, which is absent in the solid PCS. No new absorption peak appeared in the spectra of PCS-0 and PCS-15 after melt-spinning, suggesting that no new groups were generated.

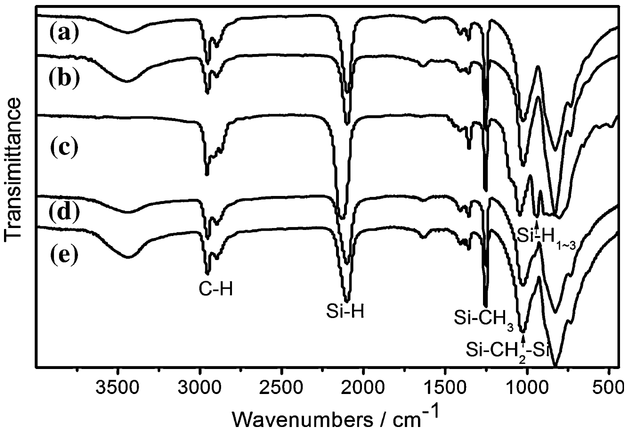

Fig. 3 FTIR spectra of (a) PCS-0 before spinning, (b) PCS-0 after spinning, (c) LPCS, (d) PCS-15 before spinning, and (e) PCS-15 after spinning

During spinning, the LPCS and the solid PCS may react, resulting in the reduction of Si–H functional groups. Since the bond energy of C–H is high, and thus the C–H bonds can be considered stable under the spinning conditions, the degree of the reaction can be semi-quantitatively assessed by the ratio of Si–H and C–H groups (SiH/CH). The area ratio of the Si–H and C–H absorption peaks in NMR spectra (Fig. 4) is calculated and shown in Table 1. Before spinning, the ratios are 0.096 for PCS-0 and 0.134 for PCS-15, because of the higher Si–H concentration in the LPCS. After spinning, the ratios decrease slightly to 0.095 for PCS-0 and 0.128 for PCS-15, indicating that most of Si–H remains intact and the LPCS is essentially stable at the melt-spinning temperature.

In the ^{1}H NMR spectra, the signal at the chemical shift of +4.4 ppm is assigned to the resonance of hydrogen from Si–H in the PCS-0 precursor [16]. The signal at +3 ppm is assigned to $Si–H_{1,2,3}$ in the LPCS [11]. Both signals appear

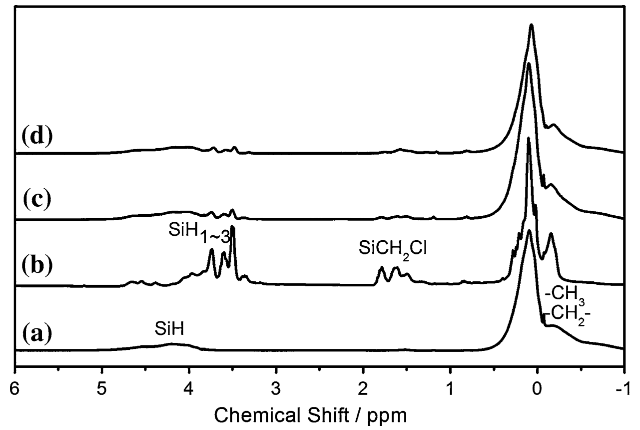

Fig. 4 ^{1}H NMR spectra of (a) PCS-0, (b) LPCS, (c) PCS-15 before spinning, and (d) PCS-15 after spinning

Table 1 SiH/CH ratio before and after melt-spinning as a function of LPCS content

SiH/CH	PCS-0	PCS-2.5	PCS-5	PCS-10	PCS-15	PCS-20
Before spinning	0.096	0.103	0.114	0.120	0.134	0.140
After spinning	0.095	0.102	0.113	0.119	0.128	0.139

in the polymer blend as expected. The ^{1}H NMR spectra are similar before and after spinning by comparing Fig. 4c and d, indicating insignificant chemical interaction between the LPCS and PCS, which is consistent with the FTIR analysis.

The molecular weight distributions of PCS, LPCS, and PCS-15 are shown in Fig. 5. The addition of the LPCS increases the low molecular weight portion. Careful examination shows that for the precursor blend, the molecular weight distribution is the superimposition of the LPCS and the PCS, indicating that the blend is a physical mixture of the two constituents and no noticeable chemical interaction has occurred. This agrees with the FTIR and NMR analysis. The high molecular weight portion increases after melt-spinning for all the fibers, because of the condensation polymerization between Si–H bonds at high temperature. The PCS-15 contains more Si–H than PCS-0, so that the high molecular weight peak is more obvious. Fortunately, this chemical interaction has no noticeably adverse effect on the spinning process.

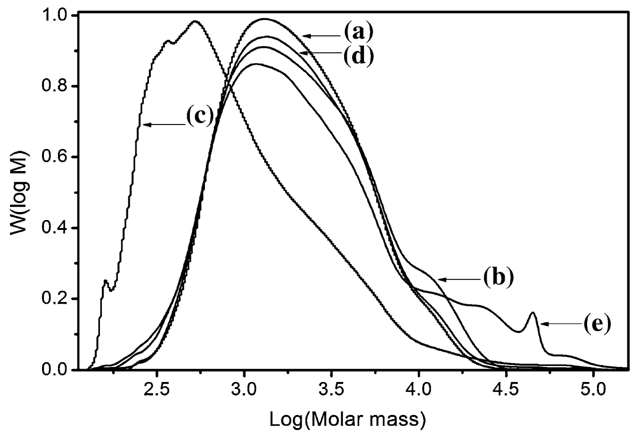

Fig. 5 GPC profiles of (a) PCS-0 before spinning, (b) PCS-0 after spinning, (c) LPCS, (d) PCS-15 before spinning, and (e) PCS-15 after spinning

Effects of LPCS on melt-spinning

Table 2 shows that the melting point and the melt-spinning temperature of the blended precursors decrease markedly with even a small amount of LPCS. With 20% LPCS, the spinning temperature is 80 °C lower than that of the solid PCS. As far as melt-spinning is concerned, lower temperature is preferred, because of reduced energy consumption, better working environment, and more importantly less polymer degradation.

For the solid PCS, fiber breakage occurs from time to time during spinning, and the average continuous fiber length is less than 500 m, while for the precursor containing only 2.5% LPCS, no breaking occurs. This clearly shows that the LPCS is beneficial to the spinning ability of the solid PCS. Idesaki et al. [10] believed that the introduction of liquid polymer into solid PCS can increase the mobility of PCS chains in the molten state and decrease the activation energy. Lower activation energy makes the viscosity of polymer melt less sensitive to temperature change, increasing the duration for the extruded filaments to remain drawable. In other words, the liquid polymer increases the maximum drawing ratio, making the extruded filaments more tolerant to drawing without breaking.

Effects of LPCS on oxidation curing

Curing is one of the most important steps in SiC fiber production. It renders the precursor fibers infusible during the subsequent pyrolysis. In this work, oxidation curing is used by heating the precursor fibers in hot air.

Oxidation curing is exothermic, raising the fiber temperature even above its melting point and making the fibers to stick together. Under the curing conditions used in this work, the PCS-20 fibers fused together, while the others retained the fiber shape. That is to say, 20% LPCS reduced the melting point too much, making the resultant fibers unable to survive the curing process.

The oxygen take-up as a function of LPCS content is shown in Fig. 6. Experimental results have indicated that 8% oxygen take-up during curing is sufficient to make the fibers infusible. At a given curing temperature, the oxygen take-up increases with the concentration of LPCS,

Table 2 Effects of LPCS on the spinning ability of solid PCS

Sample	Melting point (°C)	Spinning temperature (°C)	Continuous fiber length (m)	Average fiber diameter (μm)
PCS-0	220.4	285	489	19.6
PCS-2.5	202.2	275	Continuous	18.7
PCS-5	188.9	265	Continuous	18.2
PCS-10	155.8	245	Continuous	17.3
PCS-15	141.7	225	Continuous	15.7
PCS-20	124.8	205	Continuous	15.4

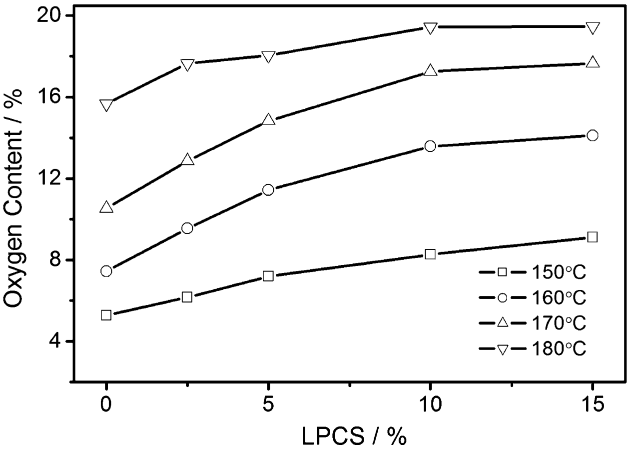

Fig. 6 Oxygen take-up as a function of LPCS content

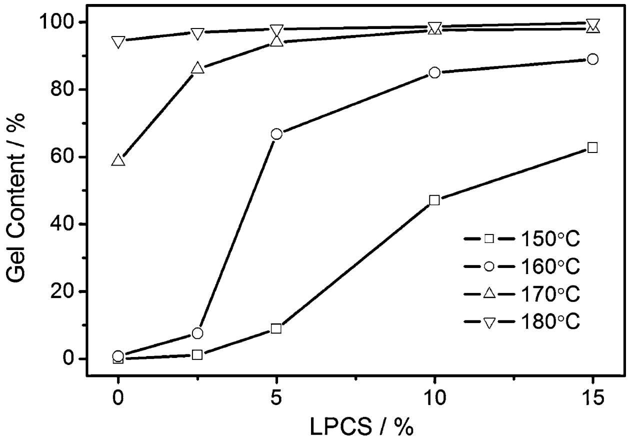

Fig. 7 Gel fraction of the cured fibers as a function of LPCS content

indicating that the LPCS speeds up the curing, or the LPCS-containing fibers can be cured effectively at lower temperature.

The positive effect of LPCS on curing is confirmed by the gel fraction of the cured fibers as shown in Fig. 7. The as-spun precursor fibers are totally soluble in xylene, and the gel fraction is nil. But after curing, the polycarbosilane molecules get cross-linked through –Si–O–Si– linkage, decreasing the fiber solubility. The greater the degree of the cross-linking is, the lower is the solubility and the higher is the gel fraction. Normally, the gel fraction of >40% will make the fibers infusible and retain the fiber shape during the subsequent pyrolysis [17, 18]. Obviously, for a given temperature, the gel fraction of the cured fibers increases rapidly with LPCS content. For the solid PCS precursor fibers, the curing temperature must be over 170 °C, while for the PCS-15, only 150 °C is needed to have the same degree of curing. The lower curing temperature has very important implication in SiC fiber production. One of the most frequently encountered problems during oxidation curing is partial melting and fusion of the fibers due to the strong exothermic reaction. The higher the curing temperature is, the more intense is the heat generated and the more probable is the partial melting. The blending of the LPCS into the solid PCS will alleviate this problem, making the control of oxidation-curing conditions less stringent.

The beneficial effect of LPCS on curing stems from the oxidation-curing mechanisms and the LPCS chemical structure. The following mechanisms have been proposed for the thermal oxidation of PCS [19]:

$$-\overset{|}{\underset{|}{\mathrm{Si}}}-\mathrm{H} \longrightarrow -\overset{|}{\underset{|}{\mathrm{Si}}}\cdot + \mathrm{H}\cdot \quad (1)$$

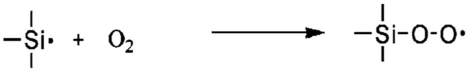

$$-\overset{|}{\underset{|}{\mathrm{Si}}}\cdot + \mathrm{O_2} \longrightarrow -\overset{|}{\underset{|}{\mathrm{Si}}}-\mathrm{O}-\mathrm{O}\cdot \quad (2)$$

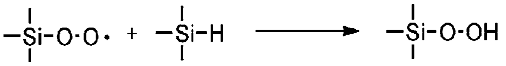

$$-\overset{|}{\underset{|}{\mathrm{Si}}}-\mathrm{O}-\mathrm{O}\cdot + -\overset{|}{\underset{|}{\mathrm{Si}}}-\mathrm{H} \longrightarrow -\overset{|}{\underset{|}{\mathrm{Si}}}-\mathrm{O}-\mathrm{OH} \quad (3)$$

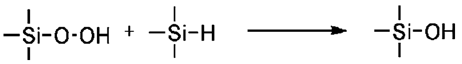

$$-\overset{|}{\underset{|}{\mathrm{Si}}}-\mathrm{O}-\mathrm{OH} + -\overset{|}{\underset{|}{\mathrm{Si}}}-\mathrm{H} \longrightarrow -\overset{|}{\underset{|}{\mathrm{Si}}}-\mathrm{OH} \quad (4)$$

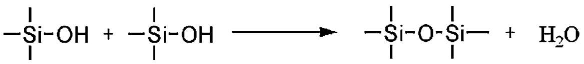

$$-\overset{|}{\underset{|}{\mathrm{Si}}}-\mathrm{OH} + -\overset{|}{\underset{|}{\mathrm{Si}}}-\mathrm{OH} \longrightarrow -\overset{|}{\underset{|}{\mathrm{Si}}}-\mathrm{O}-\overset{|}{\underset{|}{\mathrm{Si}}}- + \mathrm{H_2O} \quad (5)$$

Si–H bonds are largely responsible for the cross-linking reactions because of its much lower dissociation energy in comparison with the Si–C and C–H bonds, especially so in the initial stage or at lower curing temperature. At higher oxidation temperature, Si–CH_3 can also be oxidized to give silanol groups [19]:

$$-\overset{|}{\underset{|}{\mathrm{Si}}}-\mathrm{CH_2}\bullet + \mathrm{O_2} \longrightarrow -\overset{|}{\underset{|}{\mathrm{Si}}}-\mathrm{CH_2OO}\bullet \tag{6}$$

$$-\overset{|}{\underset{|}{\mathrm{Si}}}-\mathrm{CH_2OO}\bullet + \mathrm{RH} \longrightarrow -\overset{|}{\underset{|}{\mathrm{Si}}}-\mathrm{CH_2OOH} + \mathrm{R}\bullet \tag{7}$$

$$-\overset{|}{\underset{|}{\mathrm{Si}}}-\mathrm{CH_2OOH} \longrightarrow -\overset{|}{\underset{|}{\mathrm{Si}}}-\mathrm{OH} + \mathrm{CH_2O} \tag{8}$$

$$-\overset{|}{\underset{|}{\mathrm{Si}}}-\mathrm{CH_2OO}\bullet \longrightarrow \text{product containing } \mathrm{C{=}O} + \mathrm{O_2} \tag{9}$$

$$-\overset{|}{\underset{|}{\mathrm{Si}}}-\mathrm{OH} + -\overset{|}{\underset{|}{\mathrm{Si}}}-\mathrm{OH} \longrightarrow -\overset{|}{\underset{|}{\mathrm{Si}}}-\mathrm{O}-\overset{|}{\underset{|}{\mathrm{Si}}}- + \mathrm{H_2O} \tag{10}$$

where R represents hydrocarbon groups. The LPCS is rich in Si–H bonds as compared with PCS; therefore, the LPCS-containing precursor fibers can be effectively cured at lower temperature.

Effects of LPCS on pyrolysis and on SiC fiber properties

Figure 8 shows that the ceramic yield drops when the precursor fibers are under-cured (at 150 °C). For all the sufficiently cured fibers, the ceramic yield is ~81%. The addition of LPCS does not have an obviously adverse effect on it. This suggests that the LPCS has overwhelmingly reacted with itself or with the solid PCS during curing and pyrolysis, rather than evaporated out of the fibers. That is, the LPCS is not a temporary or fugitive component, but an essential part of the fibers.

The XRD patterns of the fibers pyrolyzed at 1250 °C are shown in Fig. 9. As the LPCS content increases, the diffraction bands corresponding to *β*-SiC crystals become more diffused, indicating poorer SiC crystallization and smaller *β*-SiC crystal size. By referring to the oxygen content, we find that the higher oxygen take-up in LPCS-containing fibers during curing is responsible. In other words, oxygen inhibits the growth of SiC crystals, in consistent with the literature [20].

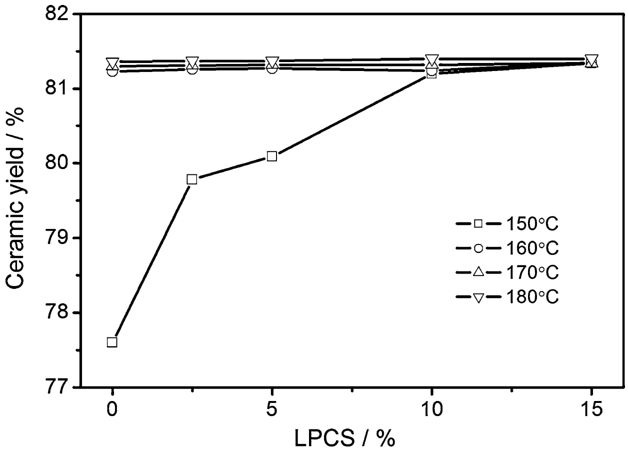

Fig. 8 Ceramic yield after pyrolysis at 1250 °C as a function of LPCS content

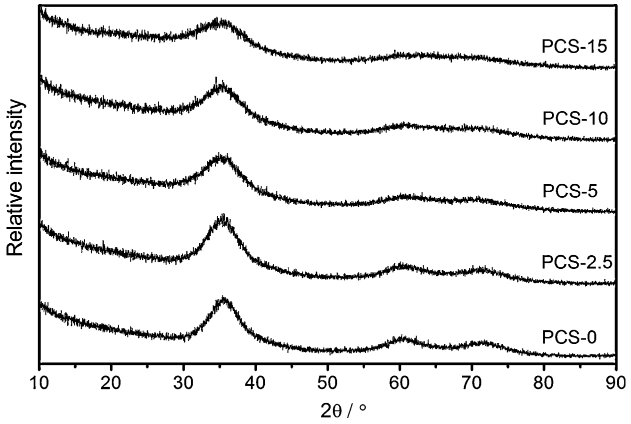

Fig. 9 XRD patterns of the fibers cured at 160 °C and pyrolyzed at 1250 °C

The tensile strength of the SiC fibers pyrolyzed in nitrogen at 1250 °C is shown in Table 3. The degree of oxidation curing must be appropriate to obtain SiC fibers with the maximum tensile strength. Either under-curing or over-curing will lead to lower fiber property. With insufficient curing, the fibers may stick together at some isolated points during pyrolysis, increasing the number density of surface defects and reducing the fiber strength. With excessive curing, the cured fibers become less flexible, making them more prone to surface damage during the subsequent handling and reducing the fiber strength.

The strength of the SiC fibers prepared from the LPCS-containing precursors is lower than the fibers from the solid PCS. This is attributed to the non-uniform oxygen distribution along the fiber radius [21]. We believe that for the solid PCS precursor fibers, oxidation is diffusion-controlled. Therefore, the oxygen can diffuse into the fibers, leading to the cured fibers with relatively uniform oxygen concentration across the fiber diameter. However, for the LPCS-containing fibers, oxidation is reaction-controlled, rather than diffusion-controlled, because of the higher concentration of the more reactive Si–H bonds. Due to the presence of oxygen-rich surface layer, further oxygen diffusion into the fiber interior is impeded, resulting in the formation of oxygen-rich surface and oxygen-deficient core, as found also in other work [21]. For the fiber core, the pyrolysis temperature of 1250 °C is optimal as far as tensile strength is concerned [22]. However, for the skin,

Table 3 Tensile strength of SiC fibers after pyrolysis at 1250 °C

Curing temperature (°C)	Tensile strength (GPa)				
	PCS-0	PCS-2.5	PCS-5	PCS-10	PCS-15
150	Fused	Fused	Fused	1.69 ± 0.35	1.58 ± 0.32
160	1.41 ± 0.58	1.46 ± 0.22	1.48 ± 0.19	1.75 ± 0.28	1.76 ± 0.26
170	2.81 ± 0.46	1.75 ± 0.11	1.75 ± 0.26	1.49 ± 0.19	1.26 ± 0.37
180	1.89 ± 0.47	1.69 ± 0.18	1.64 ± 0.19	1.28 ± 0.39	1.07 ± 0.32

extensive decomposition of the surface silicon oxycarbide phase (SiC_xO_y) will take place at this temperature, forming gaseous SiO and CO [4, 5, 23, 24]. The decomposition reaction has proved to be very detrimental to fiber strength by many previous studies [24–29].

The concentration of LPCS in the precursor seems having very little effect on the fiber strength. However, for the fibers prepared from different precursors, the maximum strength is a function of oxidation curing temperature. For the precursors containing higher LPCS, lower curing temperature is required. As explained above, generally speaking, too much oxygen take-up has an adverse effect on fiber strength. For the precursor fibers containing higher LPCS, reduced curing temperature is required to limit the oxygen take-up.

To avoid the undesirable effects of oxygen, electron beam curing under inert atmosphere is now underway. This may fully take advantage of the merits of the LPCS and circumvent its disadvantages. The results will be reported in the future.

Conclusions

A highly branched LPCS was added into a PCS to give a polymer blend. Because of their similar chemical structure and hence good compatibility, a homogeneous mixture is obtainable simply by dissolving the two polymers in hexane, and then drying under vacuum heating. The addition of the LPCS resulted in a significant drop in the spinning temperature from 285 °C (without LPCS) to 225 °C (with 15% LPCS), while the spinning ability of the polymer blend was also markedly improved over the solid PCS.

The LPCS enhanced the oxidation curing, reducing the curing temperature and hence the tendency for fiber partial melting and sticking. The reason is that the LPCS is rich in Si–H bonds in comparison with the solid PCS. The Si–H bonds are more reactive with oxygen than $Si–CH_3$ bonds. For the same amount of oxygen take-up, lower temperature is needed, making the control of oxidation conditions much less stringent.

The strength of the SiC fibers decreased owing to the presence of the LPCS. This is attributed to the oxygen-rich surface and oxygen-deficient interior structure for the ceramic fibers prepared from the polymer blend. The oxygen-rich surface suffers from decomposition during pyrolysis, creating surface defects and resulting in lower fiber strength.

Acknowledgement The project was supported by National Natural Science Foundation of China (No. 50472056, No. 50532010, and No. 50802079).

References

1. Yajima S, Hayashi J, Omori M (1975) Chem Lett 9:931
2. Yajima S, Hayashi J, Omori M et al (1976) Nature 261:683
3. Yajima S, Okamura K, Hayashi J et al (1976) J Am Ceram Soc 59:324
4. Okamura K (1987) Composites 18:107
5. Cooke TF (1991) J Am Ceram Soc 74:2959
6. Johnson DW, Evans AG, Goettler RW (1998) Ceramic fibers and coatings: advanced materials for the twenty-first century. National Academy Press, Washington, DC
7. Le Coustumer P, Monthioux M, Oberlin A (1993) J Eur Ceram Soc 11:95
8. Narisawa M, Idesaki A, Kitano S et al (1999) J Am Ceram Soc 82:1045
9. Idesaki A, Narisawa M, Okamura K et al (2001) J Mater Sci 36:357. doi:10.1023/A:1004864126085
10. Idesaki A, Narisawa M, Okamura K et al (2001) J Mater Sci 36:5565. doi:10.1023/A:1012549228826
11. Whitmarsh CK, Interrante LV (1991) Organometallics 10:1336
12. Suwardie H, Kalyon DM, Kovenklioglu S (1991) J Appl Polym Sci 42:1087. doi:10.1002/app.1991.070420422
13. Narisawa M, Shimoda M, Okamura K et al (1995) Bull Chem Soc Jpn 68:1098. doi:10.1246/bcsj.68.1098
14. Hasegawa Y, Okamura K (1986) J Mater Sci 21:321. doi:10.1007/BF01144739
15. Silverstein RM, Bassler GC, Morrill TC (1991) Spectrometric identification of organic compounds. Wiley, New York
16. Yajima S, Hasegawa Y, Hayashi J et al (1978) J Mater Sci 13:2569. doi:10.1007/BF02402743
17. Cheng XZ, Xiao JY, Xie ZF (2004) J Mater Eng 1:29
18. Wang J, Feng CX, Song YC (1998) Acta Chim Sin 56:77
19. Hasegawa Y (1989) J Mater Sci 24:1177. doi:10.1007/BF00553140
20. Ichikawa H, Teranishi H, Ishikawa T (1987) J Mater Sci Lett 6:420
21. Narisawa M, Kitano S, Okamura K (1995) J Am Ceram Soc 78:3405
22. Hasegawa Y, Iimura M, Yajima S (1980) J Mater Sci 15:720. doi:10.1007/BF00551739

23. Laine RM (1993) Chem Mater 5:260
24. Shimoo T, Sugimoto M, Okamura K (1990) J Ceram Soc Jpn 98:1324
25. Johnson SM, Brittain RD, Lamoreaux RH et al (1988) J Am Ceram Soc 71:132
26. Bouillon E, Langlais F, Pailler R et al (1991) J Mater Sci 26:1333. doi:10.1007/BF00544474
27. Shimoo T, Chen H, Okamura K (1992) J Ceram Soc Jpn 100:48
28. Vahlas C, Rocabois P, Bernard C (1994) J Mater Sci 29:5839. doi:10.1007/BF00366865
29. Vahlas C, Laanani F (1995) J Mater Sci Lett 14:1558